4ICEGE Thessaloniki-GREECE 2007

4th International Conference on
Earthquake Geotechnical Engineering
June 25-28, 2007
Paper No. 1582

DEEP IMMERSED TUNNEL SUBJECTED TO MAJOR FAULT RUPTURE DEFORMATION

Ioannis ANASTASOPOULOS[1], Nikos GEROLYMOS[1], Vasileios DROSOS[2], Rallis KOURKOULIS[2], Takis GEORGARAKOS[2], and George GAZETAS[3]

ABSTRACT

Immersed tunnels are particularly sensitive to tensile deformations such as those imposed by an outbreaking normal earthquake fault.The paper investigates the response of a proposed 70 m deep immersed tunnel to the action of a major normal fault rupture occurring in the basement rock underneath the tunnel. Non-linear finite elements are used to model the quasi-static fault rupture propagation through the soil overlying the bedrock and the ensuing interaction of the rupture with the immersed tunnel. The tunnel is modeled as a 3-D flexural beam connected to the soil through properly-calibrated non-linear interaction springs, the supports of which are subjected to the free-field fault-induced displacement. The joints between the tunnel segments are modeled with special non-linear hyper-elastic elements, while their longitudinal pre-stressing due to the 7-bar water pressure is also rigorously incorporated in the analysis. The possibility of sliding is considered through the use of special gap elements. The influence of segment length and joint properties is explored parametrically. The analysis shows that a properly designed immersed tunnel (suitable thick elastic gaskets, small length of segments, shear keys with sufficient "allowance", un-stressed tendons) can safely resist a normal earthquake fault rupture with a dislocation of 2 meters in the basement rock, 800 m underneath the tunnel. Net tension or excessive compression between the tunnel segments can be avoided with suitable design of the joints.

Keywords: Immersed tunnel, fault rupture propagation, soil–structure interaction.

INTRODUCTION

Immersed tunnels consist of a number of prefabricated floatable segments of the order of 100 m in length, usually constructed in a dry-dock, floated over a pre-excavated trench, and lowered with sinking rigs. Most of their construction is performed ashore, ensuring better quality. The connection between the segments is performed under water, using special rubber gaskets. Earthquake engineering research and practice have (over the last four decades) focused on the dynamic response of tunnels to ground oscillations (e.g. Sakurai & Takahashi, 1969 ; Hashash et al., 2001). Much less effort has been devoted to understand the effects of a rock-rupturing seismic fault on the overlying soil and subsequently on the structures founded on it. In fact, seismic codes and engineering practice had in the past invariably demanded that "buildings and important structures should not be erected in the immediate vicinity of active faults" (e.g. EC8, 1994 edition).

[1] Postdoctoral Researcher, School of Civil Engineering, National Technical University of Athens, Greece. Email: ianast@civil.ntua.gr
[2] Graduate Research Asssistant, School of Civil Engineering, National Technical University of Athens, Greece.
[3] Professor, School of Civil Engineering, National Technical University of Athens, Greece. Email: gazetas@ath.forthnet.gr

However, such a strict prohibition is difficult (and sometimes meaningless) to obey, especially in case of long structures, such as tunnels, bridges, pipelines, and embankments, which often cannot avoid crossing potentially active faults. An additional difficulty in determining the exact outcropping location of a fault, stems from the propagation of the fault rupture from the base rock to the ground surface, through the overlying soil deposit. If, where, and how large will the dislocation emerge on the ground surface, depends not only on the type and magnitude of the fault rupture, but also on the geometry and material characteristics of the overlying soils (e.g. Ambraseys & Jackson, 1984). Field observations from recent earthquakes and analytical research findings clearly suggest that the presence of a structure on top of the soil deposit may further modify the rupture path, as the latter propagates from the base rock to the ground surface — and even force it to divert from the plan of the structure. The distress of a structure subjected to a fault-induced displacement does not depend only on its location with respect to the fault outcrop in the "free-field", but also on the interplay between the propagating fault rupture, the deforming soil, and the differentially displacing structure, a phenomenon described as "Fault Rupture–Soil–Structure Interaction" (FR–SSI).

The objective of this paper is to investigate the behavior of a deep immersed tunnel under the action of a major fault rupturing underneath. The presented research is part of a feasibility study for an immersed tunnel, which is planned to cross an area of high seismicity, characterized by a maximum extensional slip rate of about 1 cm/yr. This paper develops the necessary methodology and applies it for the analysis and design of such a tunnel. It is crucial for a successful design to ensure that, within the 100 years life of the tunnel, the permanent tensile deformation due to the normal–fault rupture, will not jeopardize the water-tightness of the tunnel at any moment.

Inspired by a pre-feasibility study of a tunnel in southern Greece, a hybrid tunneling solution is examined, combining an immersed tunnel at the central deepest section of the crossing, with two bored "approach" tunnels at the two sides. The total length of the tunnel is 9.5 km, with the immersed part covering a length of 980 m (Figure 1). The central tube of 23 m x 11 m (width x height) section is designed to accommodate two-way rail traffic, with two additional tubes at both sides serving as emergency escape (in case of flood or fire) and providing the required service viaducts.

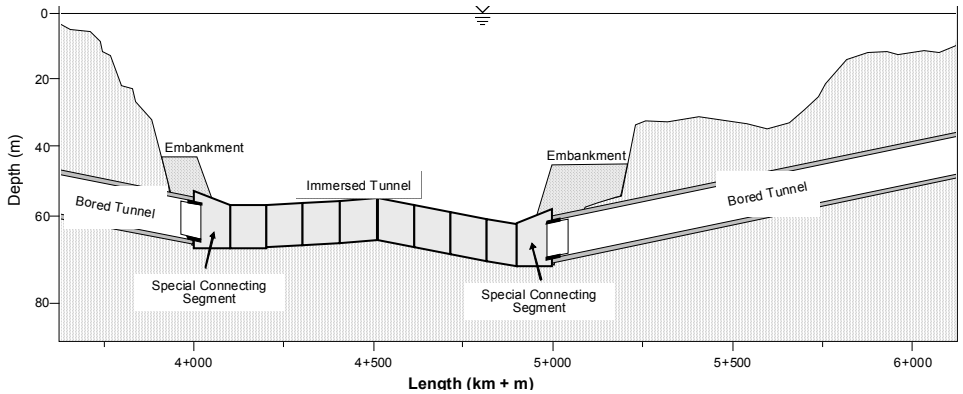

Figure 1. Longitudinal Section of the proposed tunnel

ASEISMIC DESIGN OF THE PROPOSED IMMERSED TUNNEL

As already discussed, the concrete segments will be constructed in a dry–dock , floated over the pre-excavated trench, and lowered with the help of special sinking rigs. Each segment will be lowered close to the previous one, and brought to contact using special guidance techniques. Once the two segments gain contact, the water between them will be drained, and the gina gasket will be compressed with the help of the hydrostatic water pressure acting only at the free side of the segment.
In our case, this pressure will be of the order of 7 bars, and thus the use of the largest available gina gasket is indispensable. After compression is completed, the secondary omega seal is installed. Contrary to the gina profile that requires compression to achieve water-tightness, the omega seal is

insensitive to the magnitude of compression. However, none of the above materials can transmit either shear or tension. To this end, shear keys and tendons should be installed.

The scope of this paper is to analyze the behaviour of the tunnel under fault–induced displacement. In this paper we parametrically investigate three possible segment lengths: (i) 70 m, (ii) 100 m, and (iii) 165 m. The segment length (L) determines the total number of the required immersion joints, controlling their deformation and the overall resilience of the tunnel. The modern trend is to use longer segments, since this leads to significant reduction in construction time and cost.

Besides the segment length, the type of the gina gasket was also parametrically investigated. The longitudinal deformation of the tunnel depends mainly on the properties of the gina gasket. Additionally, since the gina profile constitutes the primary seal of the tunnel, ensuring its permeability is critical. Fault–induced extension and differential settlement will unavoidably decompress at least some of the joints. The magnitude of the total de-compression is critical for the design of the tendons. Two types of joints (Figure 2) are parametrically investigated. Type A refers to the idealized behavior of the largest available gina profile, while type B is a proposed hypothetical double-sized gina-type gasket. The behavior of this hypothetical gasket provides wider deformation limits, thus permitting significant additional compression and decompression. The hyper-elastic performance of both joints is estimated from testing results of half-sized models (Kiyomiya, 1995). Our type B gasket is the logical projection. Of course, it has not yet been tested.

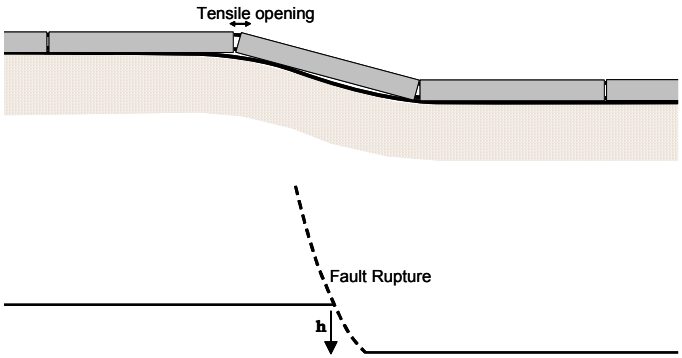

Figure 2. Description of the behaviour of the rubber gaskets. Soil deformation due to faulting causes tensile opening of the gina profile.

Finally, the "allowance" of the shear key is parametrically investigated. It is expected that this allowance will affect both the longitudinal deformation of the tunnel due to fault-induced deformation, and its transverse deformation during the strong seismic shaking. If this allowance is large enough, then the joints will allow relative displacement and rotation between two consecutive segments. On the contrary, reduced allowance makes the connection more "fixed". Two extreme alternatives are explored: 5 mm and 20 mm.

METHOD OF ANALYSIS

The finite element code ABAQUS is utilized to perform non-linear analysis of the tunnel. The layout of the model is depicted in Figure 3. The immersed tunnel is modeled as a series of beams connected to the soil through interaction springs and dashpots, and with each other through an arrangement of hyper-elastic elements simulating the behavior of the immersion joints. The tunnel segments are modeled as beam elements. Special transitional rigid elements are connected at both ends of each tunnel segment to represent the segment face, where the immersion joint is placed.

The analysis is conducted in two steps. First, in "*Step 0*" the hydrostatic pressure is applied statically to the end of the segments, to simulate the initial hydrostatic longitudinal compression. Then, in "*Step 1*" the fault-induced displacement profile is applied pseudo-statically on the model. The methodology for the analysis of fault rupture propagation, along with the resulting seabed displacement profiles, is presented in the next section.

The contact between the seabed and the tunnel is modeled using special sliding interface elements, to simulate potential sliding once the frictional capacity is exceeded. As schematically illustrated in Figure 4, in the longitudinal direction (x) the behavior of the sliding interface is that of a simple slider with the friction coefficient μ_x being the decisive parameter. The latter is computed with due consideration to buoyancy. In the transverse direction (y), the "sliding" interface is a little more complex. Since the tunnel will be back-filled, sliding is accompanied by (partial) passive failure of the backfill. Therefore, to estimate the equivalent "*friction coefficient*" μ_y, two-dimensional plane strain analysis of the tunnel cross-section was conducted (Gazetas et al., 2004).

The (immersion) joints between the tunnel segments are modeled with special non-linear "springs". In the longitudinal direction (x), the "springs" refer to the gina gasket. In the transverse direction (y), given the fact that Gina-type gaskets cannot transfer shear forces, the drift of the tunnel depends on the shear-key allowance. The behavior of the joint in this direction is modeled by special "gap" elements which do not transmit any shear force until reaching the shear-key allowance. After that, their stiffness becomes very large, depending mainly on the stiffness of the concrete in the area of the shear key.

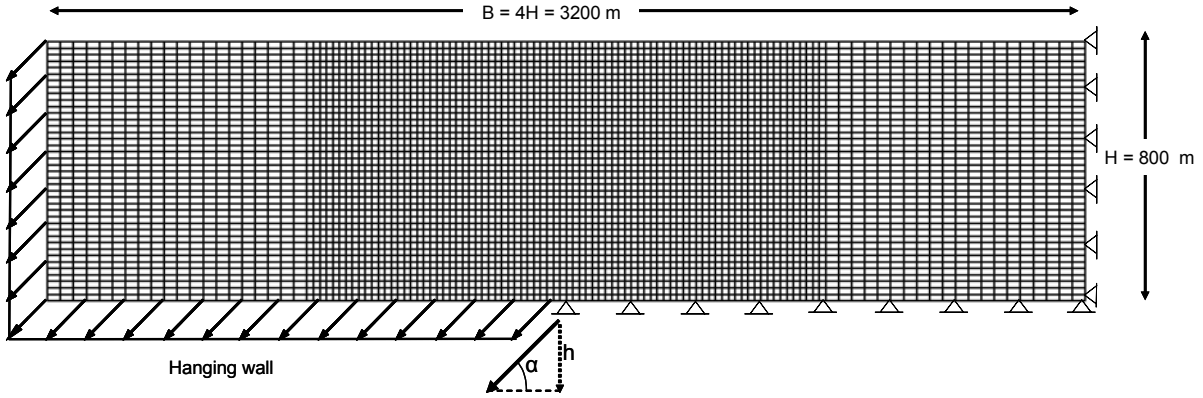

Figure 3. Finite element discretization for the plane strain analysis of fault rupture propagation through the 800 m soil sediment.

ANALYSIS OF FAULT RUPTURE PROPAGATION

As mentioned previously, the location and the magnitude of the potential dislocation of the ground surface depend not only on the type and magnitude of the fault rupture, but also on the geometry and material characteristics of the overlying soils.

The finite element method has proven successful in analyzing fault rupture propagation through soil provided that certain conditions are satisfied, such as (i) the use of a very refined mesh in the neighborhood of the potential rupture, and (ii) the use of a suitable nonlinear constitutive law for the soil (Bray, 1990; Bray et al., 1994a; 1994b). The analysis is conducted in plane strain with the use of the FE code ABAQUS. The model is displayed in Figure 4, with an H = 800 m thick soil layer, at the base of which a normal fault dipping at an angle α ruptures and produces a downward movement of vertical amplitude h. At the central 1600 m of the model, the discretization is finer, with the quadrilateral elements being 20 m x 20 m (width x height). At the two edges of the model, where the

deformation is expected to be much smaller, the mesh is coarser: 40 m x 20 m. The differential displacement is applied to the left part of the model in small consecutive steps.

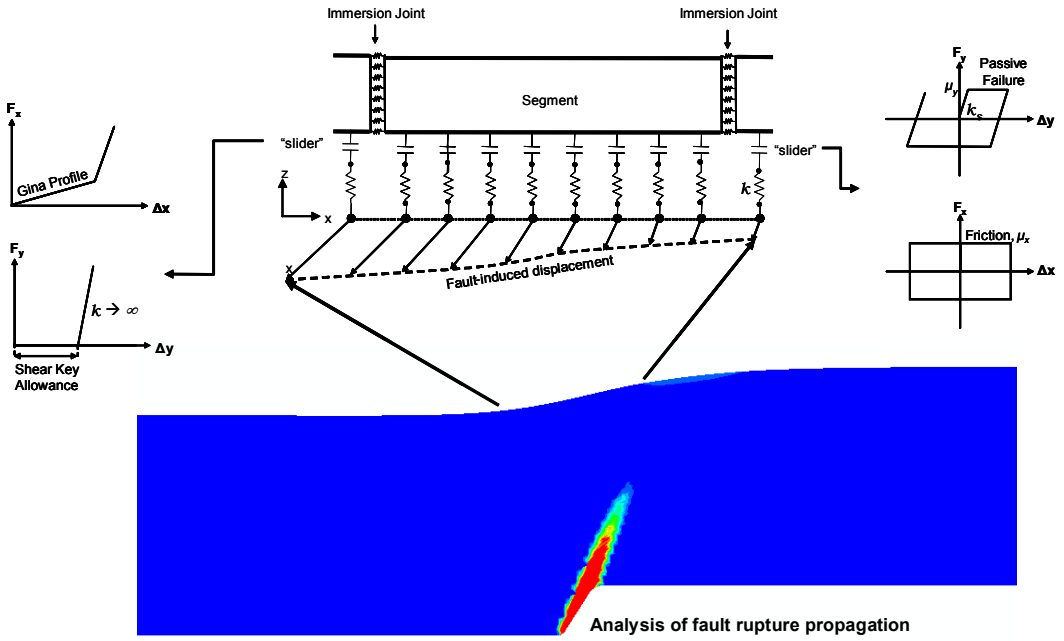

Figure 4. Finite Element Modeling of one tunnel segment. The fault-induced displacements are applied to the tunnel pseudo-statically

After a thorough review of the literature, an elastoplastic constitutive model was adopted and calibrated against test results and case histories (Anastasopoulos & Gazetas, 2007a ; 2007b): Mohr-Coulomb failure criterion, with an isotropic strain softening rule, applied to cohesion c , angle of friction φ, and angle of dilation ψ. Denoting γ_f the plastic shear strain at which soil reaches its residual strength, we consider c, φ and ψ as linearly decreasing functions of the total plastic strain until they reach their residual values c_{res}, φ_{res}, and ψ_{res}. Typical values of γ_f range from 5% to 15%. Equally important is the "yield" strain γ_y, which depends on both strength and shear stiffness.

Conservatively assuming a dip angle of 45°, a downward displacement of vertical magnitude h is imposed on the left half of the model (the "hanging" wall). A dense cohesionless soil with $\varphi = 45^o$, $\varphi_{res} = 30^o$, $\psi = 15^o$, $\psi_{res} = 0^o$, and $\gamma_y = 1.5\%$ is investigated in this study. The shear modulus G is linearly increasing with depth while γ_y is kept constant. The study has assumed $h_d = 2$ m as the design bedrock displacement (vertical component).

Figures 5a and 5b portray the profiles of vertical, Δy, and horizontal displacement, Δx, along the ground surface, for the (conservative) dense soil and for $h_d = 2$ m. The horizontal distance, d, is measured from the point of application of the bedrock displacement. Figure 6c depicts the angle of distortion β :

$$\beta = \frac{\Delta y^A - \Delta y^B}{x^A - x^B} \qquad (1)$$

where Δy^A and Δy^B is the vertical displacement at two points A and B at the ground surface, and x^A , x^B their horizontal coordinates. The horizontal strain, ε_x , along the ground surface (positive values are for tension) is depicted in Figure 5d.
The computed displacement profiles (Δx and Δy) are used as the "input" displacement to be imposed on the tunnel model. The tensile deformation causes decompression of the joints, while the bending

deformation decompresses some of the immersion joints and possibly further compresses some other. Since the maximum bending and tensile deformation does not occur at the same location, we identify two tunnel–fault rupture relative positions (Figure 5) :

(1) *Position 1* : the center of the tunnel coincides with the location of max β , and
(2) *Position 2* : the center of the tunnel coincides with the location of max ε_x .

The "prediction" of the "worst-case scenario" is not straightforward. Therefore, both positions are investigated.

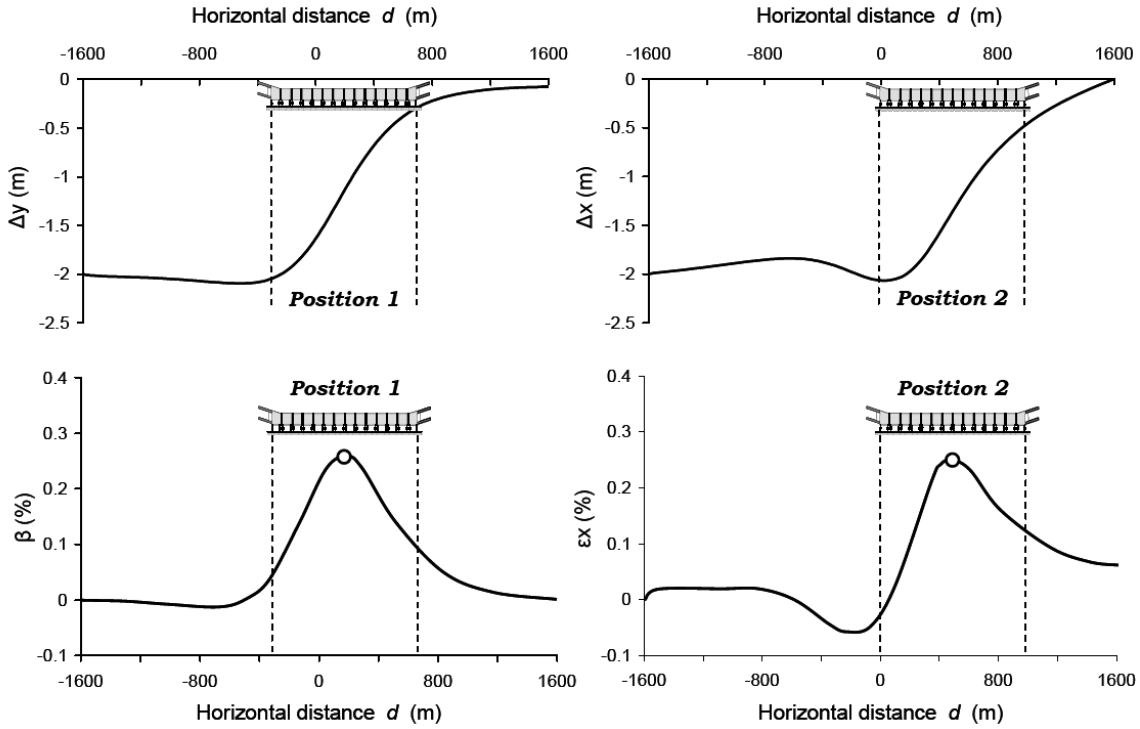

Figure 5. Fault rupture propagation analysis results for a fault rupture α = 45^o in dip and bedrock displacements h_d = 2 m, for the idealized dense sandy soil : (a) horizontal displacement Δ_x, (b) vertical displacement Δ_y, (c) angular distortion β, and (d) horizontal strain ε_x at the seabed.

EFFECTS OF FAULT RUPTURE ON THE IMMERSED TUNNEL

Typical results of a complete analysis are portrayed in Figure 6, in terms of joint deformation, sliding displacement, bending moments and axial forces. Figure 6a corresponds to segment length L = 70 m with a type A gasket, while Figure 6b to segment length L = 100 m with the type B gasket. Results for L = 165 m have been also examined but are not shown herein: with such a large length the tunnel cannot sustain the total developing stressing without several joints experiencing net tension — a precarious situation indeed. Similarly, the "allowance" in the shear keys plays only a minor role; thus, results are given only for a single value (5 mm) of this "allowance". In all cases the results presented herein correspond to the position "2" scenario since this proved to be the most critical case.
The following conclusions are drawn:

1. The application of the fault–induced tensile displacement decompresses all the joints, with those near the middle of the tunnel experiencing the greatest tension with more pronounced being the decompression when the segment length is 100 m (Figure 6b).
2. This initial slippage is greater in the middle of the tunnel, where the maximum tensile deformation ε_x takes place. Increasing the segment length only marginally increases the

maximum sliding displacement (from 7.5 cm to 9 cm in the middle of the tunnel for segment lengths L = 70 m and L = 100 m respectively).

3. At first, the axial force exhibits an initial "pre-stressing" of 160 MN due to hydrostatic compression (Step 0). Then the application of the fault–induced deformation (Step 1) causes longitudinal decompression of the tunnel, reducing the axial force (N) significantly. In the case of the 70 m segments, N drops from 160 MN to only 30 MN near the middle. The increased segment length makes things worse: the initial compression is completely lost, and even some (small) tensile stressing develops (at point C).
4. The fault-induced deformation is responsible for the development of longitudinal bending moments, M_y. With L = 70 m, at point "A" a moment of 70 MNm is developed while point "C" (at the opposite end) is almost unaffected by the imposed displacement (M_y = 5 MNm). The increase of L to 100 m leads to an increase of the longitudinal bending moment.

(a)

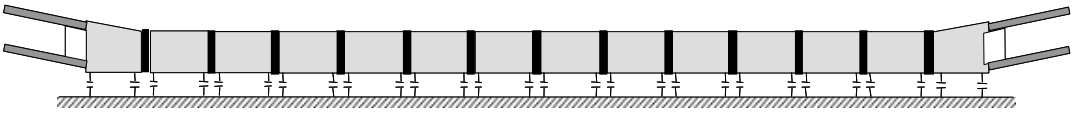

	Joint Decompression (cm)	Segment Slippage (cm)	N (MN)	M (MNm)
A	1	0	-130	-70
B	16	7.5	-30	40
C	10	5	-50	5

(b)

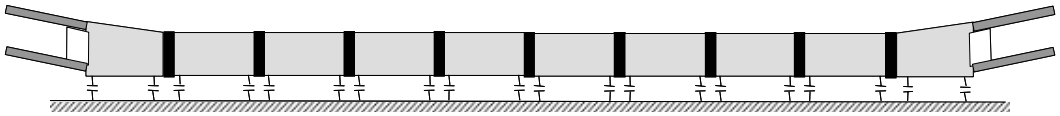

	Joint Decompression (cm)	Segment Slippage (cm)	N (MN)	M (MNm)
A	4	1	-100	-150
B	21	-9	-80	-10
C	14	-2	10	140

Figure 6. Joint deformation, sliding displacement, axial forces and bending moments after the fault induced displacements for (a) 70 m segments and (b) 100 m segments (fault at Position 2, type B gasket, and 5 mm shear-key allowance)

CONCLUSIONS

Several conclusions of practical significance can be drawn from the presented study (including additional parametric results not shown here for the sake of brevity):

1. A properly designed immersed tunnel (suitable thick elastic gaskets, small length of segments, shear keys with sufficient "allowance", un-stressed tendons) can safely resist a normal fault rupture with a dislocation (offset) of 2 meters in the basement rock, 800 m underneath the tunnel.
2. The initial hydrostatic compression of each gasket is independent of segment length, or of total number of the joints. Increasing the total number of the joints (or decreasing the segment length) leads to increased total initial hydrostatic compressive deformation of the tunnel. To ensure water-tightness, the initial compression of the Gina gaskets must be significant. When subjected to fault–induced tensile displacements, their ability to remain water-tight is highly dependent on the extent of the initial compression to avoid developing net tension.
3. Increasing the thickness of the Gina gasket leads to greater initial hydrostatic compression: from 17 cm for the Type A gasket, to 28.5 cm for the Type B. Since the tectonic deformation is mainly tensile, this increase of the initial compressive deformation leads to higher margins of safety.

ACKNOWLEDGEMENT

The authors would like to acknowledge the financing of this research project by the Greek Railway Organization (OSE). The third author would also like to acknowledge the State Scholarships Foundation of Greece (IKY) for financial support. We also thank Messieurs Hans van Italie, Hendrik Postma, Gerard H. van Raalte, P. van der Burg, and Royal Boskalis S.A. for kindly offering their comments and suggestions on construction-related issues. Our "computational" belief on the feasibility of the project was greatly enhanced by their real life experience.

REFERENCES

Ambraseys, N. & Jackson, J., (1984), "Seismic movements", *Ground movements and their effects on structures.* Ed. P.B. Attewell and R.K. Taylor, Surrey University Press, pp. 353-380.

Anastasopoulos, I. (2005), *Fault Rupture–Soil–Foundation–Structure Interaction (FR–SFSI)*, Ph.D. Dissertation, School of Civil Engineering, National technical University, Athens, pp. 570.

Anastasopoulos I., & Gazetas G. (2007a), "Foundation–structure systems over a rupturing normal fault. Part I : Observations after the Kocaeli 1999 earthquake", *Bulletin of Earthquake Engineering* (in print).

Anastasopoulos I., & Gazetas G. (2007b), "Foundation–structure systems over a rupturing normal fault. Part II : Analysis of the Kocaeli case histories", *Bulletin of Earthquake Engineering* (in print).

Bray, J.D. (1990), *The effects of tectonic movements on stresses and deformations in earth embankments*, Ph.D. Dissertation, University of California, Berkeley.

Bray, J.D., Seed, R.B., Cluff, L.S., and Seed, H.B. (1994a), "Earthquake fault rupture propagation through soil", *Journal of Geotechnical Engineering,* ASCE, Vol. 120, No.3, pp. 543-561.

Bray, J.D., Seed, R.B., and Seed, H.B. (1994b), "Analysis of earthquake fault rupture propagation through cohesive soil", *Journal of Geotechnical Engineering,* ASCE, Vol. 120, No.3, pp. 562-580.

EC8 (1994) *Eurocode 8* : Structures in seismic regions. Part 5 : Foundations, retaining structures, and geotechnical aspects. Brussels : Commission of the European Communities.

Gazetas, G., Anastasopoulos, I., Gerolymos, N., Drosos, V., Kourkoulis, R, and Georgarakos, P. (2004), *Dynamic analysis of the Rion-Antirrion tunnels and preliminary immersion joint design*, Technical Report, Vol. 1 – 4, Athens, July 2004.

Hashash, Y.M.A., Hook, J.J., Schmidt, B., and Yao, J.I-C. (2001) "Seismic design and analysis of underground structures", *Tunneling and Underground Space Technology*, Vol. 16, No. 2, pp. 247-293.

Kiyomiya, O. (1995) “Earthquake-resistant design features of immersed tunnels in Japan”, *Tunnelling and Underground Space Technology*, Elsevier, Vol. 10, No. 4, pp. 463-475.
Sakurai, A., Takahashi, T. (1969), Dynamic stresses of underground pipeline during earthquakes. Proceedings of the Fourth World Conference on Earthquake Engineering.